Optimization of the Electron Cooling by SIN Tunnel Junctions

L. Kuzmin[1], I. Agulo, M. Fominsky[1,2], A. Savin[3], M. Tarasov[1,2]

[1] Chalmers University, Institute of Microtechnology and Nanoscience, Gothenburg, Sweden, kuzmin@fy.chalmers.se,

[2] Institute of Radio Engineering and Electronics, Moscow, Russia,

[3] Helsinki University of Technology, Finland

Abstract. We report on optimization of the electron cooling by SIN tunnel junctions due to advanced geometry of superconducting electrodes (quadrant shape) and very effective Au traps just near the junctions (≈0.5 μm) at temperatures from 25 mK to 500 mK. The maximum decrease in temperature of about 200 mK has been observed from temperatures 300-350 mK. We used 4-junction geometry with Al-AlOx-Cr/Cu (or Cr/Al) tunnel junctions and Au traps. Effective electron cooling was realized due to the improved geometry of the cooling tunnel junctions (superconducting electrode) and effective normal metal traps to decrease reabsorption of quasiparticles after removing them from normal metal. The maximum cooling effect was increased from dT=-50 mK (ordinary cross geometry) to -130 mK (improved geometry of superconducting electrodes) and to dT=-200 mK (improved geometry of superconducting electrodes and effective metal traps).
Heating peak (instead of cooling) near zero-cooling voltage has been observed practically for all samples at temperatures lower than 150 mK. For higher cooling voltages close to superconductoing gap, the heating was converted to cooling with decreased amplitude. The leakage resistance of the tunnel junctions gives rather good explanation of these heating peaks. The phonon reabsorption due recombination of quasiparticles in superconducting electrodes give additional improvement of theoretical fitting but could not explain the heating peak. Anomalous zero-bias resistance peak has been observed for all tested structures. The peak is explained by Coulomb blockade of tunneling in transistor-type structure with relatively small tunnel junctions. The works on electron cooling are devoted to development of a cold-electron bolometer (CEB) with capacitive coupling by SIN tunnel junctions to the antenna for sensitive detection in THz region. Direct electron cooling of absorber will play crucial role for supersensitive detection in presence of the realistic background power load.

1. Introduction

In the last decade superconducting detectors have become the most sensitive radiation detectors of Sub-mm, Infrared, and Optical radiation with an estimated ultimate sensitivity down to 10^{-20} W/Hz$^{1/2}$ [1]. Ultra-low-noise bolometers are required for space-based astronomical observations. The proposed NASA missions, SPIRE, SPIRIT and SPECS, will determine highest level of requirements for bolometers for nearest future.

The detector goal is to provide a noise equivalent power less than 10^{-20} W/Hz$^{1/2}$ [2] over the 40 – 500 μm wavelength range in a 100x100 pixel detector array. No one existing technology could satisfy these requirements. The proposed concept of Cold-Electron Bolometer (CEB) with direct electron cooling [3,4] could be a good candidate to realize a limit performance of the detector. The concept is based on the effect of nonequilibrium electron cooling by SIN tunnel junctions [5,6]. In contrast to cooling the membrane with detector on it[7], we propose the CEB with very effective *direct electron cooling* of the absorber [3,4]. The CEB gives opportunity to remove incoming background power from supersensitive region of absorber to return system to lowest temperature state (T_e) to achieve the fundamental limit NEP [8]

$$NEP^2 = 2\,P_0\,kT_e\,. \qquad (1)$$

For P_0=10 fW and T_e=50 mK we would get the limit NEP=1*10^{-19} W/Hz^{-19}.
The first step in this development is realization of a strong electron cooling. This work has been devoted to optimization of superconducting electrodes and normal metal traps.

2. Model

The operation of SINIS structure can be analyzed using heat balance equation [9,10]:

$$P_{cool}\,(V, T_e, T_{ph}) + \Sigma\Lambda\,(T_e^5 - T_{ph}^5) = P_0 + \frac{V^2}{R_l} + \beta\,\frac{I}{e}\Delta\,. \qquad (2)$$

Here, cooling power

$$P_{cool}(V, T_e, T_{ph}) = \frac{1}{e^2 R}\int dE N_S(E)(E - eV)\left[f_N(E - eV) - f_S(E)\right], \qquad (3)$$

$\Sigma\Lambda(T_e^5 - T_{ph}^5)$ is the heat flow from electron to the phonon subsystems in the normal metal, Σ is a material constant, Λ - a volume of the absorber, T_e and T_{ph} are, respectively, the electron and phonon temperatures of the absorber; $P_{cool}(V, T_e, T_{ph})$ is cooling power of the SIN tunnel junctions; P_0 is the background power load, V^2/R_l is power dissipation in leakage resistance of the junction R_l [11], and the last term accounts for power flow backtunneling of quasiparticles and reabsorbtion of phonons emitted by quasiparticle recombination [12]. In simulation we have used 5th and 6th order of heat flow from phonons. Energy diagram (Fig. 1a) illustrate the principle of the electron cooling and the problem of reabsorption of the phonons emitted by quasiparticle recombination.

3. Cooling experiments

The first step was the fabrication of the normal metal traps. Au was chosen as the material for the traps fabricated in the same vacuum cycle as the contact pads. The pattern for the traps and the pads were formed using photolithography. Au was thermally evaporated up to a thickness of 600 Å. The next step was the fabrication of the tunnel junctions and the absorber. The structures were patterned by e-beam lithography and the metals were thermally evaporated using the shadow evaporation technique. The Al (superconductor) was evaporated at an angle of about 60° up to a thickness of 650Å and oxidized at a pressure of 10^{-1} mbar for 2 minutes. A Cr/Cu (1:1) absorber of a total thickness of 750 Å was then evaporated directly perpendicular to the substrate.
Figure 1b shows the configuration of the electrodes with advanced geometry of the two outer (cooling) junctions and with normal metal traps. The cooling junctions have a normal state resistance R_N equal to 0.86 kΩ, while the two inner junctions have R_N equal to 5.3 kΩ. The inner junctions have a simple cross geometry, where a section of the

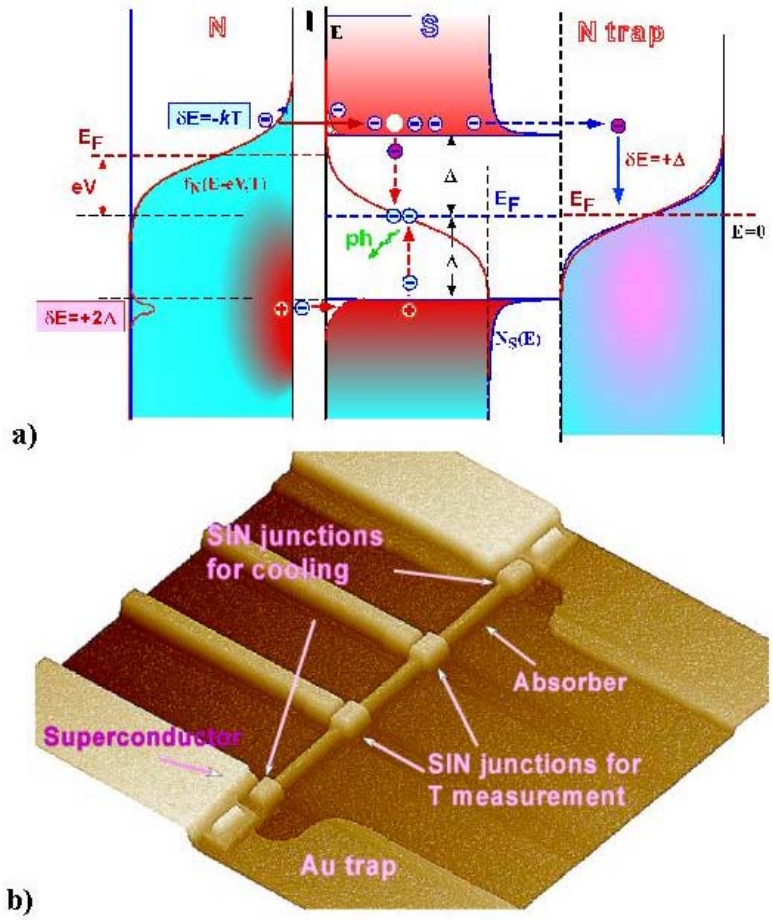

Figure 1. a) Energy diagram illustrates the principle of the electron cooling and the problem of reabsorption of the phonons after recombination of the quasiparticles. The normal metal trap is introduced to avoid this reabsorption. (b) The AFM image of the cooling structure made by shadow evaporation technique. The Au trap was evaporated prior to the evaporation of the Al-AlOx-Cr/Cu tunnel junctions.

normal metal absorber overlaps the thin Al electrodes. The area of overlap, which is equivalently the area of each of the tunnel junction, is equal to 0.2 x 0.3 μm^2. The structure of the outer junctions is such that the ends of the normal metal absorber overlap with a corner of each of the Al electrodes, which has a much larger area compared to the middle Al electrodes. The area of each of these junctions is 0.55 x 0.82 μm^2. The purpose of the larger area Al electrode is to give more space for quasiparticle diffusion compared to the middle Al electrode with simple cross geometry. In the described structure, the two outer and inner junctions have a R_N equal to 0.85 kΩ and 5.4 kΩ, respectively. The volume of absorber was 0.18 μm^3.

A bias cooling current is applied through the outer junctions and the absorber. These tunnel junctions act as the cooling junctions, and therefore serve to decrease the electron temperature of the absorber. To determine the electron temperature, the voltage across the inner junctions is measured. This voltage is then calibrated as a function of temperature, and shown in figure 2. A small current bias is applied to these junctions. The bias has to be optimal to obtain the maximum linear voltage response on temperature, and yet not too large so as to disturb the cooling process in the absorber.

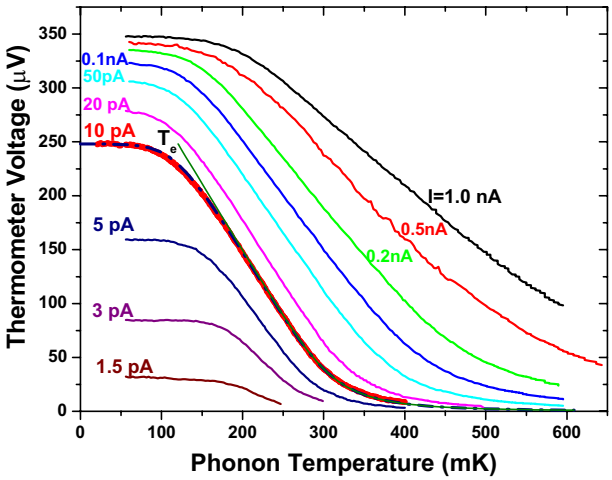

Figure 2. Calibration of the thermometer junction: the voltage in dependence on phonon temperature. The theoretical fit and the electron temperature are shown for the main calibration curve chosed for cooling experiment with the bias current of 10 pA,.

For lower currents it's limited by leakage resistance and for larger currents by overheating of the absorber by power dissipation in leakage resistance of tunnel junctions. The optimal applied bias was 10 pA. The Fig 2 shows the theoretical fit and the electron temperature for calibration curve with this bias current. The fit was obtained using equations (2,3) with power load 9.5 fW and leakage resistance 17 MΩ per junction.

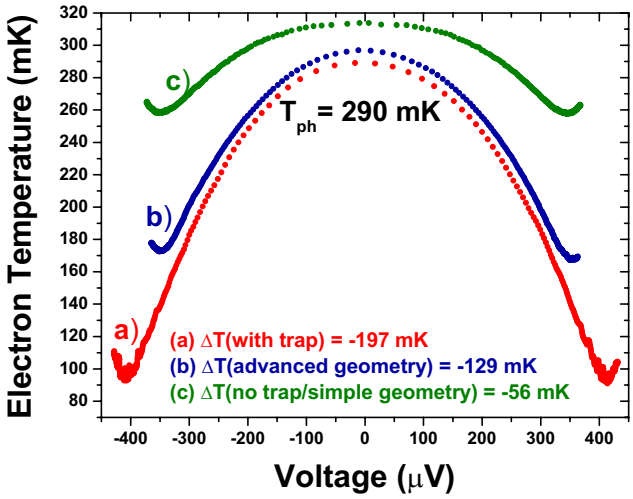

Figure 3. The main cooling curves: electron temperature of absorber as a function of the voltage across the cooling SIN tunnel junctions for (a) advanced geometry of superconducting electrodes and effective Au traps, (b) advanced geometry of superconducting electrodes without traps, and (c) ordinary cross geometry.

The Figure 3 shows the main results with the electron cooling for different geometry. The experimental calibration curve of measured voltage on temperature from Fig. 2 was used for conversion of the thermometer voltage to the temperature. The temperature as a function of the cooling voltage is shown in Fig. 3 for various combinations of geometry of superconducting electrodes and effective Au traps (a-c). We can see strong influence of advanced geometry (b) in comparison with usual cross

geometry (a) due to more open way for quasiparticles out of junction area. The further improvement (a) in comparison with (b) is obtained due to close position of traps (≈0.5 μm) near the tunnel junction.

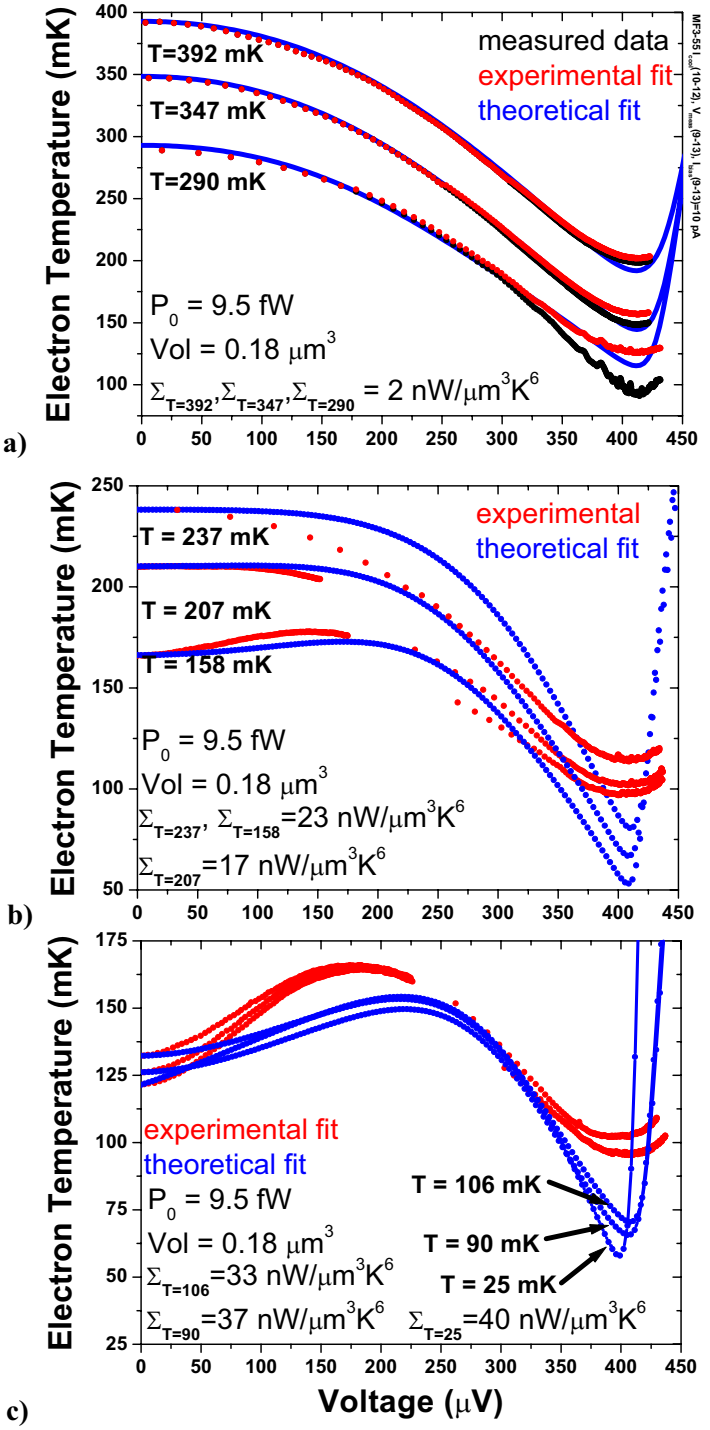

Figure 4. The main cooling curves and theoretical fit: electron temperature as a function of the voltage across the cooling junctions for different temperature regions. The fit parameters are show on the graphs, the leakage resistance was taken from the experiment R_l=1MΩ, and reabsorption coefficient, β=0.02, was found from the fit.

Comparison with theory for cooling curves is shown in Fig. 4. In Fig. 4a we used for experimental curves both the experimental calibration curve of measured $V(T_{ph})$ from Fig. 2 and theoretical estimation of $V(T_e)$ shown in the same figure. For Fig. 4b,c we used only calibration curve $V(T_e)$ giving better coincidence with theory.

The best coincidence is obtained for curves with phonon temperature 300-400 mK. The fit parameters are show in the graphs. The leakage resistance was taken from the experiment R_l=1MΩ, and reabsorption coefficient, β=0.02, was found from the fit. Heating peak (instead of cooling) near zero-cooling voltage has been observed at temperatures lower than 150 mK practically for all samples. For higher cooling voltages close to superconductoing gap, the heating was converted to cooling with decreased amplitude. The leakage resistance of the tunnel junctions gives rather good fitting for this heating peak. The phonon reabsorption due recombination of quasiparticles in superconducting electrodes gives additional improvement of theoretical fitting but could not explain the heating peak without leakage resistance.

4. Anomalous zero-bias resistance peak

In addition to the V(T) calibration of the thermometer, we used the zero-bias resistance dependence $R_0(T)$. We determined R_0 of thermometer junctions using modulation technique with lock-in amplifier [13]. For the beginning, the $R_d(V)$ has been measured (Fig. 5). If we start from higher voltages, the measurements show typical increase of the resistance up to 150 μV due to increase of the subgap resistance, and, then, flattering due to leakage resistance (17 MΩ).

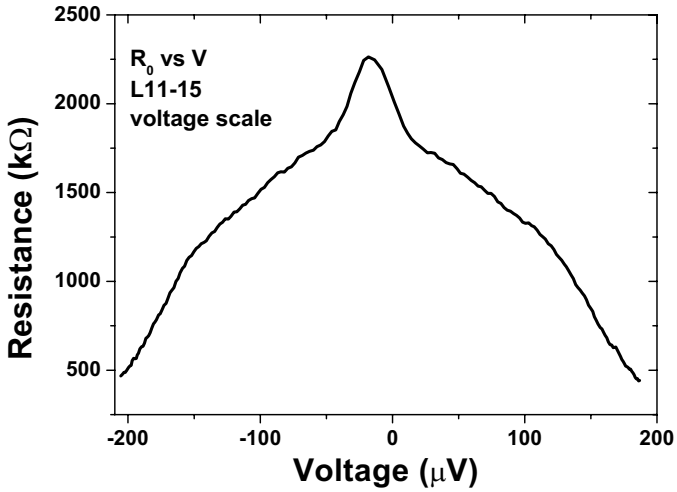

Figure 5. Voltage dependence of the differential resistance, R_d, of the cooling junctions. The dependence show some flattering due to leakage resistance (±150 μV) and, then, anomalous zero-bias resistance peak at low tvoltages. The peak is interpreted as Coulomb blockade peak due to SET transistor-type geometry of the cooling structure.

Unpredictable behaviour has been observed near zero voltage: an anomalous zero-bias peak appeared there and it is typical for all structures. To clear up the situation, the $R_0(T)$ has been measured for both temperature measuring (9-13) and cooling (D10-12, L11-15) junctions (Fig. 6). The curves for 9-13 junction shows exponential increase of resistance from higher to lower temperatures, then unpredictable change of slope to linear dependence near T=260 mK, and then flattering near 120 mK. The curves 10-12 and 11-15 show opposite behaviour: exponential increase down to 200 mK, then flattering, and

then again increase (!) near zero voltages. Flattering can be easy explained by leakage resistance but other features are rather puzzling.

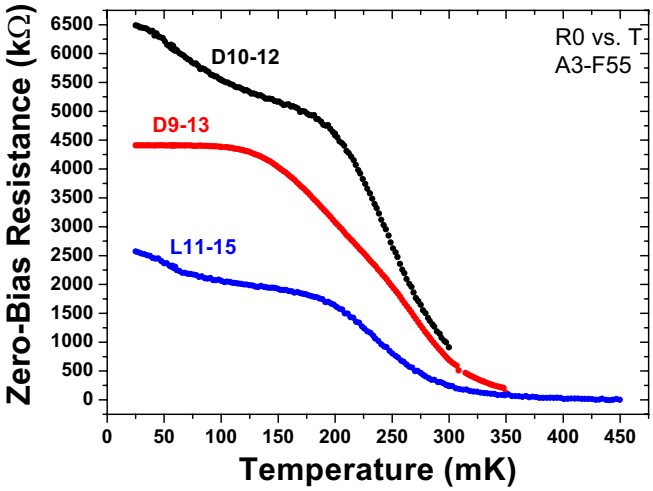

Figure 6. Temperature dependence of the zero-bias resistance, R_0, of the thermometer junctions (D9-13) and cooling junctions (D10-12 and L11-15). The dependences show flattering due to leakage resistance and increase of anomalous peak at low temperatures (different for smaller D9-13 junctions). The peak is interpreted as Coulomb blockade peak due to SET transistor-type geometry of the cooling structure.

The only explanation we manage to find is due to Coulomb blockade of tunneling in transistor-type structure with relatively small tunnel junctions. The estimation of typical parameters of the structures gives the following figures:

Sample	Area, μm^2	C, pF	V_{CB}, μV	ΔVpeak.exp, μV	T peak, mK	$T_{exp\text{-}V(T)}$, mK
D10-12	0.45	0.02	5.7	10	110	80
D9-13	0.06	0.0018	44	20	220	260
L11-15	0.45	0.02	5.7	22	260	80

Table 1. Parameters of SINIS cooling structure (junctions D9-13), two SIN thermometer junctions (D9-13), and bolometer structure (L11-15). V_{CB} is Coulomb blockade voltage determined from junctions capacitance and absorber capacitance, ΔVpeak.exp - experimental width of peak, Tpeak - temperature of smearing proportional to the ΔVpeak.exp, and $T_{exp\text{-}V(T}$ - experimental value of smearing of peak from Fig. 6.

The dependences $R_0(V)$ in the Fig. 7 show typical heating near zero voltage and then cooling for higher voltages. The right axis shows these data converted to electron temperature using the experimental calibration curve of Fig. 6 for thermometer junctions D9-13. Accuracy near minimum temperature is rather low due to flattering of calibration curve near minimum temperature caused by leakage resistance. This reason decreases an accuracy of temperature determination using $R_0(T)$ in comparison with V(T). The Coulomb blockade peak gives additional difficulties in calibration and theoretical fitting for this calibration curve for more correct determination of the electron temperature.

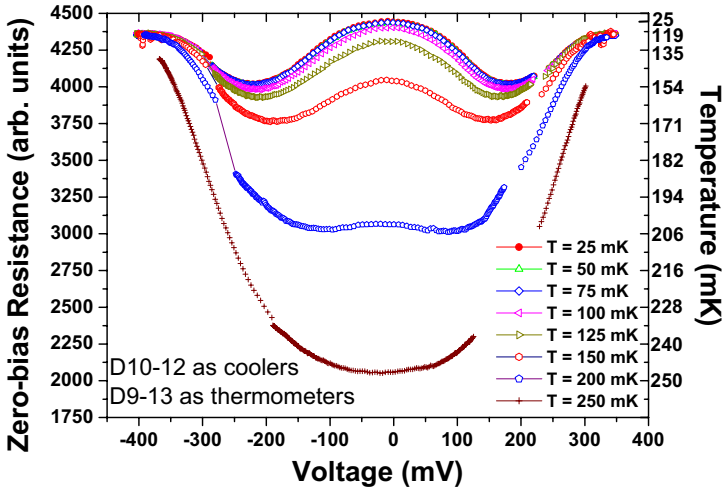

Figure 7. The zero-bias resistance, R_0, of the thermometer junctions (D9-13) and the electron temperature of the absorber as a function of the voltage across the cooling SIN tunnel junctions (D10-12) for various phonon temperature. Experimental relation $R_0(T)$ from Fig. 6 was used for estimation of the electron temperature of the absorber.

Conclusions

The optimization of the electron cooling by SIN tunnel junctions has been done for the advanced geometry of the superconducting electrodes (quadrant shape) and very effective Au traps just near the junctions (≈0.5 μm) at temperatures from 25 mK to 500 mK. The maximum decrease in temperature of about 200 mK has been observed for combination of these two improvements.

Heating peak (instead of cooling) near zero-cooling voltage at temperatures lower than 150 mK observed practically for all samples has been explained by the leakage resistance of the junctions. The phonon reabsorption due recombination of quasiparticles in superconducting electrodes gives additional improvement of theoretical fitting but could not explain alone the heating peak.

Anomalous zero-bias resistance peak has been observed for all tested structures. The peak is explained by Coulomb blockade of tunneling in transistor-type structure with relatively small tunnel junctions.

References

1. A. Bitterman, Superconductor & Cryoelectronics, Vol. 12, No. 2, (1999) 17.
2. D Leisawitz et al., “Scientific motivation and technology requirements for the SPIRIT and SPECS far-infrared/submillimeter space interferometers”, SPIE 2000.
3. L. Kuzmin, *Physica B: Condensed Matter*, **284-288**, (2000) 2129.
4. L. Kuzmin, I. Devyatov, and D. Golubev.. Proc. of SPIE, v. 3465, pp. 193-199 (1998).
5. M.Nahum, J.M.Martinis, Appl. Phys. Lett., v. 65, N 23, 3123 (1994).
6. M.Leivo, J.Pecola and D.Averin. Appl. Phys. Lett., v. 68, 1996 (1996).
7. J. Pekola, D. Anghel, T. Suppola, et al., *Applied Physics Letters*, **76**, (2000) 2782.
8. L. Kuzmin. to be published.
9. D. Golubev and L. Kuzmin. J. of Appl. Phys. **89**, 6464-6472 (2001).
10. L. Kuzmin and D. Golubev. Physica C **372-376**, pp 378-382 (2002).
11. A. Savin, M. Prunnila, J. Ahopelto, et al., Physica B, (2003).
12. J. Jochum, C. Mears, S. Golwala, et al., J. Appl. Phys. **83**, 3217 (1998).
13. A. Manninen, J. Suoknuuti, M. Leivo, J. Pekola. Appl. Phys. Lett. **74**, 3020 (1999).